J. Fluid Mech. (1985), *vol.* 161, *pp.* 199–216
Printed in Great Britain

On phase velocity and growth rate of wind-induced gravity–capillary waves

By KLAARTJE VAN GASTEL, PETER A. E. M. JANSSEN AND GERBRAND J. KOMEN
Royal Netherlands Meteorological Institute, De Bilt, The Netherlands

(Received 28 August 1984 and in revised form 11 June 1985)

The generation and growth of gravity–capillary waves ($\lambda \approx 1$ cm) by wind are reconsidered using linear instability theory to describe the process. For all friction velocities we solve the resulting Orr–Sommerfeld equation using asymptotic methods. New elements in our theory, compared with the work of Benjamin (1959) and Miles (1962), are more stress on mathematical rigour and the incorporation of the wind-induced shear current. We find that the growth rate of the initial wavelets, the first waves to be generated by the wind, is proportional to u_*^3.

We also study the effect of changes in the shape of the profiles of wind and wind-induced current. In doing this we compare results of Miles (1962), Larson & Wright (1975), Valenzuela (1976), Kawai (1979), Plant & Wright (1980) and our study. We find that the growth rate is very sensitive to the shape of the wind profile while the influence of changes in the current profile is much smaller. To determine correctly the phase velocity, the value of current and current shear at the interface are very important, much more so than the shape of either wind or current profile.

1. Introduction

Recently interest in generation, growth and equilibrium of gravity–capillary waves has been renewed owing to the growing importance of remote sensing of the sea surface. Microwave-radar backscatter is determined largely by the energy density of waves with wavelengths of the order of 4–40 cm (Raney *et al.* 1985). In order to ascertain the energy density one needs knowledge of sources and sinks of energy and of kinematical quantities like advection and refraction.

In this study only part of this intricate process is considered. We concentrate on the initial generation and growth of gravity–capillary waves under the influence of the wind.

Most of the recent studies on this subject use the linear-instability theory as presented by Miles (1957). In 1959 Benjamin made an analytical study of the flow over a wavy boundary. He looked at the flow over a rigid surface, in this way decoupling the flows in the two media. Although he noted the possibility of generalizing this theory to the flow over a fluid and determining growth rates, he did not carry out such a programme. Miles (1962) did apply Benjamin's theory to the growth of gravity–capillary waves by wind. He used a linear–logarithmic flow in air, the profile of which is drawn in figure 1. In accordance with Benjamin he assumed the water to be at rest. It may be noted that these two flows do not satisfy the equation for continuity of shearing stress at the boundary of two fluids.

Valenzuela (1976) numerically solved the equations using a coupled wind–current

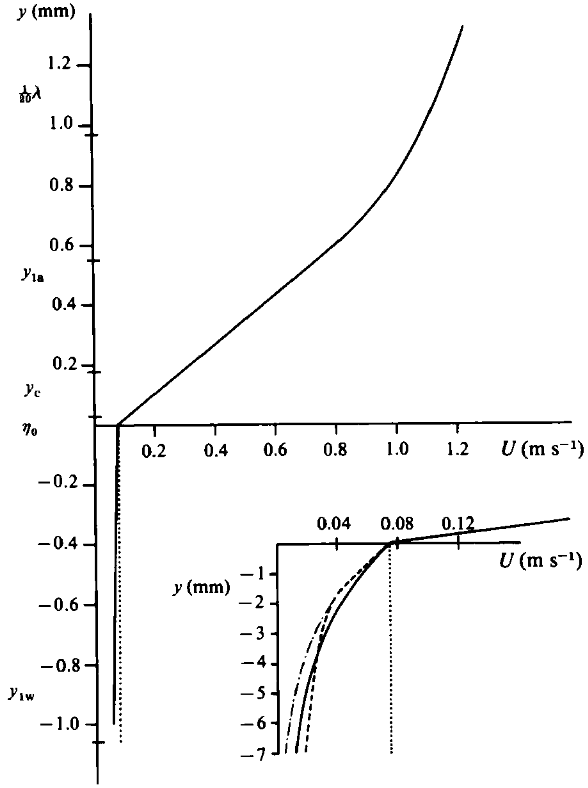

FIGURE 1. Wind speed and current as a function of height. In air a linear–logaritimic profile is drawn; in water: . . . . . , Miles' constant profile (Miles took $U_0 = 0$, in this figure we took $U_0 = 0.75$ m s^{-1}); – – – –, Valenzuela's linear–logarithmic profile; —·—, Kawai's error-function-like profile; ——, our exponential profile. On the vertical scale typical values for various quantities are indicated. λ is a wavelength, y_{1a} a thickness of the viscous sublayer in air, y_c a critical height, η_0 a wave amplitude and y_{1w} a thickness of the viscous sublayer in water as assumed in Valenzuela's profile.

system satisfying the continuity equations. For the wind as well as for the current he assumed a linear–logarithmic profile.

Kawai (1979*a*) extended the research to the generation of gravity–capillary waves by combining numerical and experimental work. He measured the flow at the moment the initial wavelets appeared and their growth rate, phase velocity and frequency. His numerical work describes these measurements. He used a coupled wind–current system, an error-function-like current profile (drawn in figure 1) and the usual wind profile.

In the next section our analytical analysis is presented. We use the linear–logarithmic profile in air and an exponential profile in water (figure 1). We have chosen this profile because it closely resembles Kawai's profile and because it allows for an exact solution of the Rayleigh equation. We briefly discuss the derivation of the Orr–Sommerfeld equation plus boundary conditions as a description of the growth of gravity–capillary waves. We then solve these equations asymptotically. Asymptotic analysis makes sense because the density of air is small compared to the density of water and because reasonably large Reynolds numbers can be defined in air and water. We find expressions for the phase velocity and growth rate of the waves.

It is inherent with the asymptotic methods that we are able to indicate to what order each expression is correct. This is an improvement on the wave-growth theories of both Benjamin and Miles. We are even able to indicate the order of the errors in Miles' expression for the growth. Another improvement of our analysis is that the main flows satisfy the continuity equations. This means that formal justification for our expressions exists, in contrast to the cases of Benjamin and Miles. Numerical results of our analysis are given in §3. We also study how sensitive the phase velocity and growth rate are to changes in shape of the profiles of wind and current, by comparing the results of Miles, Valenzuela, Kawai and our study: each is based on a different profile. For verification we use the experimental laboratory results of Kawai (1979*a*), Larson & Wright (1975) and Plant & Wright (1980).

2. Theory

2.1. *Methods and equations*

The growth of waves on the interface of water and air can be seen as the perturbation of the equilibrium consisting of a plane interface and uniform basic flow in air and water. Physically, the description would be as follows. The wind sets in and after a few seconds the upper layer of the water starts to drift with the wind. These flows, both strongly sheared near the interface, are unstable and after another few seconds ripples start to appear (see Kawai 1979*a*). In this initial stage the growth of the waves is exponential; after a further few seconds other mechanisms come into effect and saturation sets in. In a final stage the wind and current profile would be modified by the constant flow of energy from the air towards the waves. In this paper we confine ourselves to the initial stage of wave growth, where instability and viscous damping are the only energy sources. Keeping this in mind a mathematical description of the growth of the waves can be given. Growth is then described as an instability of the equilibrium in the normal-mode analysis. For simplicity the situation is assumed to be uniform in one horizontal direction: as we are interested in plane-parallel flow this does not diminish the possibility of finding growth (Drazin & Reid 1982, p. 155). In a later section the description of the wind and the wind-induced current must be chosen. Here we only assume the basic flows to be shear flows satisfying at the interface the usual continuity equations of normal and tangential velocity, shearing stress and normal pressure (Batchelor 1981, p. 148–150). The equation for the continuity of shearing stress will be of importance. It reads:

$$\mu_a U_a'(0) = \mu_w U_w'(0), \tag{1}$$

where μ is the viscosity, U is the velocity of the basic flow in the horizontal direction and a prime denotes differentation with respect to ξ, a dimensionless height coordinate equal to the product of wavenumber (see (6)) and height y. The subscripts a and w stand for air and water respectively.

We are interested in the deviation $\eta(x,t)$ of the interface from equilibrium, where x is the non-trivial horizontal coordinate and t the time. To calculate η we introduce a perturbation stream function ψ. It is assumed to have a wave-like nature:

$$\psi(x,y,t) = \phi(y)\, e^{ik(x-ct)}. \tag{2}$$

It will be seen from (6) that η has the same x- and t-dependence; thus k is the wavenumber and c the phase velocity.

The equations for ϕ, the height-dependent part of the stream function, can be easily derived from the five conservation laws and the equation of state (Batchelor 1981,

p. 164) which together govern the fluid motion. Additional assumptions we made are: temperature and density are constant; gravity is the only body force present; and turbulence and other nonlinear features are neglected, although they enter indirectly through the background profile. Here it may be added that surface tension, which cannot be neglected for the short waves of interest here, is a conservative force like gravity. Thus we know beforehand that these two forces influence the frequency and not the growth of the waves. Surface tension is not a body force but enters through the boundary conditions. The governing equations then become the Orr–Sommerfeld equation plus linearized boundary conditions. These boundary conditions express the vanishing of the wave-induced disturbance at large heights and the continuity conditions at the interface.

In dimensionless form the equations read (see Valenzuela 1976; Kawai 1979*a*):

$$W\left(\frac{\mathrm{d}^2}{\mathrm{d}\xi^2}-1\right)\phi - W''\phi = -\mathrm{i}\epsilon\left(\frac{\mathrm{d}^2}{\mathrm{d}\xi^2}-1\right)^2\phi, \quad \xi \neq 0; \tag{3}$$

$$\left.\begin{aligned}
&\phi_\mathrm{a} = \phi_\mathrm{w}, && (4a)\\
&W'_\mathrm{a}\phi_\mathrm{a} - W_0\phi'_\mathrm{a} = W'_\mathrm{w}\phi_\mathrm{w} - W_0\phi'_\mathrm{w}, && (4b)\\
&\delta\frac{\epsilon_\mathrm{a}}{\epsilon_\mathrm{w}}\left[\left(1-\frac{W''_\mathrm{a}}{W_0}\right)\phi_\mathrm{a}+\phi''_\mathrm{a}\right] = \left(1-\frac{W''_\mathrm{w}}{W_0}\right)\phi_\mathrm{w}+\phi''_\mathrm{w}, && (4c)\\
&\delta\left[\left(W'_\mathrm{a}+\frac{g}{u_*^2 kW_0}\right)\phi_\mathrm{a}-(W_0-3\mathrm{i}\epsilon_\mathrm{a})\phi'_\mathrm{a}-\mathrm{i}\epsilon_\mathrm{a}\phi'''_\mathrm{a}\right] &&\\
&\quad = \left(W'_\mathrm{w}+\frac{g}{u_*^2 kW_0}\right)\phi_\mathrm{w}-(W_0-3\mathrm{i}\epsilon_\mathrm{w})\phi'_\mathrm{w}-\mathrm{i}\epsilon_\mathrm{w}\phi'''_\mathrm{w}+\frac{Tk}{\rho_\mathrm{w}u_* W_0}, && (4d)
\end{aligned}\right\}\ \xi = 0;$$

$$\xi \rightarrow \pm\infty: \quad \phi \rightarrow 0, \quad \phi' \rightarrow 0. \tag{5}$$

Here u_* is the friction velocity in air (see §2.3), W is a dimensionless velocity, $W = U - c$, and W_0 is the value of W at $\xi = 0$, the air–water interface. The gravitational acceleration is g, T is the surface tension and ρ the density. δ and ϵ are dimensionless constants: $\delta = \rho_\mathrm{a}/\rho_\mathrm{w}$ and $\epsilon = \nu k/u_*$, the inverse of a Reynolds number.

Finding the growth of a particular wave is now translated into solving the problem outlined above. To completely determine the problem we need boundary conditions or initial values in x and t. As we are interested in temporal growth rates we take periodic boundary conditions in x and initial values for ϕ at a given time. This implies that k is real and that c is solved as a function of k. When one is interested in spatial growth, i.e. growth with fetch, the roles of x and t are reversed and initial values for given x and boundary conditions in t are taken (Kawai 1979; Drazin & Reid 1982, pp. 152–153). The imaginary part of c determines the growth rate, as can be seen from the equation for the interface (which can be derived from the kinematical boundary condition):

$$\eta = \frac{-\phi_\mathrm{a}(0)}{W_0}\,\mathrm{e}^{\mathrm{i}k(x-ct)}. \tag{6}$$

To find c as a function of k the profiles of wind and current have to be specified; then the problem is completely determined. We next solve the Orr–Sommerfeld equation in air and water separately using asymptotic methods (see, for instance, Drazin & Reid 1982, chapter 4). The boundary conditions at infinity are applied and the solutions are coupled with the aid of the continuity equations. Throughout we will use the fact that δ, ϵ_a and ϵ_w are small parameters:

$$\delta \ll 1, \quad \epsilon_a \ll 1, \quad \epsilon_w \ll 1. \tag{7a,b,c}$$

2.2. *Basic flow and perturbation stream function in water*

As mentioned in the introduction the basic flow in the water is taken to be

$$U_w = U_0 e^{\lambda\xi}, \quad \lambda = \frac{\delta u_*}{\epsilon_w U_0}. \tag{8a,b}$$

We take the water flow to be time independent. This is consistent with the experimental results of Kawai (1979); he found the flow to depend on time but on a much larger scale than the growth of the waves.

Substitution of (8) in the Orr–Sommerfeld equation enables us to find the perturbation stream function ϕ_w in water. We write ϕ_w as a sum of two independent solutions. These will be called the inviscid and viscid solution respectively, ϕ_{iw} and ϕ_{vw}, as one is in first order a solution of the inviscid Rayleigh equation and the other is relatively large in regions where viscosity is important. We normalize the solution to unity at the surface:

$$\phi_w = C\phi_{iw} + D\phi_{vw}, \quad \phi_w(0) = 1. \tag{9}$$

Normalization of ϕ_w is possible because the set of equations (3)–(5) does not depend on the amplitude of the perturbation (substitution of $\hat{\phi} = \alpha\phi$ yields exactly the same equations). For convenience we also normalize the two independent solutions:

$$\phi_{iw}(0) = \phi_{vw}(0) = 1.$$

The inviscid solution can be found by a formal expansion of ϕ_{iw} and ξ in ϵ_w ($\epsilon_w \ll 1$!). To first order this yields:

$$\left.\begin{aligned} \phi_{iw} &= \phi_{iw0} + i\epsilon_w \phi_{iw1} + O(\epsilon_w^2), \\ \phi_{iw0} &= e^{\xi}\frac{F(p,q;r;U/c)}{F(p,q;r;U_0/c)}, \\ \phi_{iw1} &= \xi K\phi_{iw0} + \hat{\phi}_{iw1}. \\ p = \frac{1}{\lambda} + \left(1+\frac{1}{\lambda^2}\right)^{\frac{1}{2}}, &\quad q = \frac{1}{\lambda} - \left(1+\frac{1}{\lambda^2}\right)^{\frac{1}{2}}, \quad r = 1 + \frac{2}{\lambda}, \end{aligned}\right\} \tag{10}$$

The function $\hat{\phi}_{iw1}$ is a complicated expression. Upon inspection we find

$$\hat{\phi}_{iw1}(0) = \hat{\phi}'_{iw1}(0) = 0,$$

which is the only result required below. Here K is an integral over the total depth of a differential operator working on ϕ_{iw0}; the exact form of the operator and an explicit expression for K are given in the Appendix (A 1)–(A 3). F is the hypergeometric function (see Abramowitz & Stegun 1965).

The viscid solution varies on a scale of $\epsilon_w^{\frac{1}{2}}$ (Drazin & Reid 1982). It can be found by a WKB approximation:

$$\left.\begin{aligned} \phi_{vw} &= \exp\int_0^{\xi} f\,d\xi'; \\ f &= -(i\epsilon_w)^{-\frac{1}{2}}(-W)^{\frac{1}{2}} - \frac{5}{4}\frac{W'}{W} + O(\epsilon_w). \end{aligned}\right\} \tag{11}$$

Note that (9)–(11) give the complete solution of the Orr–Sommerfeld equation satisfying the boundary conditions at infinite depth.

2.3. *Basic flow and perturbation stream function in air*

We have taken the usual linear–logarithmic wind profile (figure 1):

$$\left.\begin{aligned} U_{\mathrm{a}} &= \frac{\xi u_*}{\epsilon_{\mathrm{a}}} + U_0, \quad \xi \leqslant \xi_1; \\ U_{\mathrm{a}} &= U_1 + U_0 + \frac{u_*}{\kappa}\,(\alpha - \tanh \tfrac{1}{2}\alpha), \quad \xi \geqslant \xi_1; \\ \sinh \alpha &= \frac{2\kappa}{\epsilon_{\mathrm{a}}}\,(\xi - \xi_1); \\ \xi_1 = r\epsilon_{\mathrm{a}}, &\quad \kappa = 0.4, \quad U_1 = ru_*. \end{aligned}\right\} \tag{12}$$

The value of r determines the thickness of the viscous sublayer. All that is known about its value is that it is of the order of unity (Monin & Yaglom 1971). In the literature on the growth of gravity–capillary waves values of 5 and 8 prevail (Miles 1962; Valenzuela 1976; Kawai 1979). We have taken $r = 5$. All the essentials of the analysis are independent of this choice; only the values of the growth rates are larger for larger r.

From (8) and (12) it can be deduced that the condition for continuity of shearing stress at the interface, i.e. (1), is fulfilled. To solve the Orr–Sommerfeld equation with (12) as the basic flow we again separate the solution ϕ_{a} into an inviscid and a viscid part:

$$\phi_{\mathrm{a}} = A\phi_{\mathrm{ia}} + B\phi_{\mathrm{va}}, \quad \phi_{\mathrm{a}}(0) = 1, \quad \phi_{\mathrm{ia}}(0) = \phi_{\mathrm{va}}(0) = 1. \tag{13}$$

The results of Kawai (1979) concerning the phase velocity indicate that it is reasonable to assume that the critical height ξ_{c} (defined by $U_{\mathrm{a}}(\xi_{\mathrm{c}}) = c$) is beneath the top of the viscous sublayer:

$$\xi_{\mathrm{c}} < \xi_1. \tag{14}$$

This implies that the Rayleigh equation has no singularities. The zeroth-order expansion of the inviscid solution (which is the solution of the Rayleigh equation) can then be calculated numerically without complications. We used the method described by Janssen & Peeck (1985). It will be important in the following to note that:

$$\left.\begin{aligned} &\text{for } n \text{ odd} && \phi_{\mathrm{ia}}^{n} = \begin{cases} O(1/\epsilon_{\mathrm{a}}) & \text{for } 0.007 \leqslant \epsilon_{\mathrm{a}} \leqslant 0.02, \\ O(1) & \text{for } 0.06 \leqslant \epsilon_{\mathrm{a}} \end{cases} \\ &\text{and for } n \text{ even} && \phi_{\mathrm{ia}}^{n} = O(1). \end{aligned}\right\} \tag{15}$$

Note the two ranges for the order of magnitude of ϕ_{ia}^{n} when n is odd. For intermediate ϵ_{a}, i.e. $0.02 \leqslant \epsilon_{\mathrm{a}} \leqslant 0.06$, the order of ϕ_{ia}^{n} is also intermediate. For $u_* \approx 0.15$ m s^{-1} the minimum value for ϵ_{a} of 0.007 corresponds to wavelengths where capillary effects become unimportant. It is the smallest value for ϵ_{a} that we have considered.

Equation (14) also implies that in the inner viscous layer (a thin layer around the critical height; for an exact definition see Drazin & Reid 1982) the profile can be approximated by $U_{\mathrm{a}} = (\xi u_*/\epsilon_{\mathrm{a}}) + U_0$. In the inner viscous layer, which includes the interface, the viscid solution varies on a scale of $\epsilon_{\mathrm{a}}^{\frac{2}{3}}$. It is given to order $\epsilon_{\mathrm{a}}^{\frac{2}{3}}$ by the second integral of the Airy function (Drazin & Reid 1982):

$$\left.\begin{aligned}\phi_{\mathrm{va}} &= \frac{\mathrm{Ai}\,(\zeta, 2)}{\mathrm{Ai}\,(\mathrm{i}^{\frac{1}{3}}\epsilon_{\mathrm{a}}^{\frac{1}{3}}\,W_0, 2)}, \quad \xi < \xi_{\mathrm{c}} + \epsilon_{\mathrm{a}}^{\frac{1}{3}};\\ \zeta &= \frac{\mathrm{i}^{\frac{1}{3}}}{\epsilon_{\mathrm{a}}^{\frac{1}{3}}}\,[\xi + \epsilon_{\mathrm{a}}\,W_0], \quad \text{phase}\,(\mathrm{i}^{\frac{1}{3}}) = \tfrac{1}{6}\pi.\end{aligned}\right\} \tag{16}$$

The function $\phi'_{\mathrm{va}}(\zeta_0)$ has often been tabulated and plotted (e.g. Benjamin 1959). It is related to the Tietjens function D_{T}:

$$D_{\mathrm{T}}(\|\,\zeta_0\,\|) = -(\epsilon_{\mathrm{a}}^{\frac{2}{3}}\,\phi'_{\mathrm{va}}(\zeta_0))^{-1}.$$

2.4. *Phase velocity and growth rate*

Application of the remaining boundary conditions (4*b–d*) to the stream functions in air and water yields expressions for A, B, C, D and c. We find

$$\left.\begin{aligned}B &= \begin{cases} O(\epsilon_{\mathrm{a}}^{-\frac{1}{3}}) & \text{for } 0.007 \leqslant \epsilon_{\mathrm{a}} \leqslant 0.02,\\ O(1) & \text{for } 0.06 \leqslant \epsilon_{\mathrm{a}},\end{cases}\\ D &= \begin{cases} O(\delta\epsilon_{\mathrm{a}}^{-\frac{2}{3}}) & \text{for } 0.007 \leqslant \epsilon_{\mathrm{a}} \leqslant 0.02,\\ O(\delta\epsilon_{\mathrm{a}}^{-\frac{1}{3}}) & \text{for } 0.06 \leqslant \epsilon_{\mathrm{a}},\end{cases}\\ A &= 1 - B, \quad C = 1 - D.\end{aligned}\right\} \tag{17}$$

The cause of the two distinct ranges in the orders of magnitude of A, B and D is their dependence on ϕ'_{ia}. In principle, a third range also occurs when $1/\epsilon_{\mathrm{a}} - W_0\,\phi'_{\mathrm{ia}} = O(1/\epsilon_{\mathrm{a}})$. However, we have checked that this does not occur for $\epsilon_{\mathrm{a}} \geqslant 0.007$.

To find the phase velocity c we introduce an expansion for it. Many powers and cross-terms of the small parameters δ, ϵ_{a} and ϵ_{w} appear in the equations. However, we find that it is possible to define

$$\left.\begin{aligned}c &= c_0 + c_1 + c_2 + \dots,\\ \frac{c_1}{c_0} &= O(\delta\epsilon_{\mathrm{a}}^{-\frac{4}{3}}, \epsilon_{\mathrm{w}}),\\ \frac{c_2}{c_1} &= O(\epsilon_{\mathrm{w}}^{\frac{1}{2}}, \epsilon_{\mathrm{a}}^{\frac{2}{3}}, \delta).\end{aligned}\right\} \tag{18}$$

The order estimates depend on the relative magnitude of the small parameters. We have indicated several possibilities; the largest of these determines the accuracy of the expression.

The approximations to the phase velocity c_0 and c_1 can be expressed as follows:†

$$c_0 = U_0 - \frac{1}{2\phi'_{\mathrm{iw0}}}\left[\lambda U_0 - \left((\lambda U_0)^2 + 4\phi'_{\mathrm{iw0}}\left(\frac{g}{k} + \frac{Tk}{\rho_{\mathrm{w}}}\right)\right)^{\frac{1}{2}}\right], \tag{19a}$$

$$c_1 = u_*\,\frac{-\mathrm{i}\epsilon_{\mathrm{w}}\,\mathscr{H} + \delta(\mathscr{P} - \mathrm{i}m\mathscr{T})}{\mathscr{N}}. \tag{19b}$$

The terms ϕ'_{iw0}, $\mathscr{H}$, $\mathscr{P}$, m, $\mathscr{T}$ and $\mathscr{N}$ are given in the Appendix (A 3)–(A 8). $\mathscr{H}$ represents the effects of viscosity and shear flow in water; its value is approximately 4.

† We are only interested in gravity–capillary waves and neglect the possibility of finding Tollmien–Schlichting waves, although they are also solutions of the equations (Miles 1962).

$\mathscr{P}$ and $\mathscr{T}$ are respectively the complex amplitude of normal pressure and shear stress of the air on the surface. They have been made dimensionless by dividing by $-\rho_a k u_*^2 \eta W_0$. $\mathscr{P}$ is dominated by the term $-\mathrm{i}\epsilon_a B\phi_{va}'''$ and $\mathscr{T}$ by $\epsilon_a B\phi_{va}''$. m, the coefficient of $\mathscr{T}$, depends on properties of the flow in the water, for the case of no flow it equals 1. $\mathscr{N}$ also depends on the water flow and has a value of about 2.

The growth rate of the energy β is given by

$$\beta = 2k \operatorname{Im} c. \tag{20a}$$

As $c = c_0 + c_1$ and c_0 is real this implies

$$\beta = 2k \operatorname{Im} c_1. \tag{20b}$$

Equation (20a) follows immediately from (6) and the definition of energy density for surface waves.

To get some feeling of what (19) implies we first consider the case $U_a = U_w = \text{const.}$ Then (19) simplifies to

$$c_0 = U_0 + \left(\frac{g}{k} + \frac{Tk}{\rho_w}\right)^{\frac{1}{2}}, \quad \mathscr{H} = 4, \quad \mathscr{P} = \left(\frac{g}{ku_*^2 W_0^2} - 1\right) W_0, \quad m = 1, \quad \mathscr{T} = 0, \quad \mathscr{N} = 2.$$

c_0 is now the familiar expression for the phase velocity of free waves. $\mathscr{H}/\mathscr{N}$ describes viscous damping and $\mathscr{P}/\mathscr{N}$ the correction to the phase velocity due to the renormalization of the gravity force (see Whitham 1974, p. 445). Here it may also be noted that when $\delta = 0$ growth is impossible, as c_0 is real. This was found numerically by Kawai (1977), who studied the possibility of the instability of a sheared current generating waves.

The effect of the shear in the water is to decrease c_0 and the damping due to changes in $\mathscr{H}$ and $\mathscr{N}$. The shear in the air together with its viscosity have two effects. One is that the pressure is shifted in phase relative to the surface waves, thereby making growth possible (Miles 1957 was the first to determine the phase shift of the pressure). The other is that the tangential stress $\mathscr{T}$ is now non-zero.

Another interesting simplification is that of a wind profile that is linear up to infinity. This is quite realistic for the very short waves ($\xi_c \ll \xi_1$). Moreover, this flow allows for an exact solution of the Orr–Sommerfeld equation in terms of the Airy function. This was already known to Mises (1912a, b) and Hopf (1914) and perhaps the solution is of even earlier date. For the profile

$$U_a = \frac{\xi u_*}{\epsilon_a} + U_0 \tag{21}$$

expression (16) for ϕ_{va} becomes valid at all heights and ϕ_{ia} becomes exactly

$$\phi_{ia} = \mathrm{e}^{-\eta}, \quad \eta = \xi + \epsilon_a W_0.$$

Equation (19) remains the same but the pressure can now be given explicitly:

$$\mathscr{P} = \frac{g}{ku_*^2 W_0} + \lambda \tilde{U}_0 - W_0 \phi_{iw0}' + \frac{\phi_{va}'''}{\epsilon_a W_0 \phi_{va}'}. \tag{22}$$

Here $\tilde{U}_0 = U_0/u_*$; ϕ_{va}''' and ϕ_{va}' can be found in the Appendix, (A 21)–(A 22).

Both the shear stress and the normal pressure appear in (19b). However, the effect of the stress on the growth is much smaller than the effect of the pressure. This can be deduced by noting that $m = O(1)$ and comparing the leading terms of $\mathscr{P}$ and $\mathscr{T}$: $-\mathrm{i}\epsilon_a B\phi_{va}'''$ and $\epsilon_a B\phi_{va}''$. Then note that for both ϕ_{va}'' and ϕ_{va}''' the real and imaginary part are of the same order and that $\|\phi_{va}''\|$ is an order $\epsilon_a^{-\frac{2}{3}}$ smaller than $\|\phi_{va}'''\|$.

Miles (1962) also expressed the growth in terms of approximations to the pressure and shear stress:†

$$c_{1\mathrm{M}} = \tfrac{1}{2}[-\mathrm{i}\epsilon_{\mathrm{w}}\,4+\delta(\mathscr{P}_{\mathrm{M}}-\mathrm{i}\mathscr{T}_{\mathrm{M}})]\,u_{*}. \tag{23}$$

However, there are two important differences between Miles' expression and ours. Firstly, Miles' expression is formally invalid since the shearing stress of the basic flows is discontinuous at the surface; Miles assumed $U_{\mathrm{w}} \equiv 0$. In the next section it will be seen that the numerical results of (23) are, however, satisfactory (this was also shown by Valenzuela 1976). Secondly, Miles approximated the pressure and shearing stress on physical rather than mathematical grounds (actually, Benjamin 1959 made these approximations and Miles adopted them). Therefore he was not able to indicate to what order his expressions were correct. Using our mathematical analysis we can estimate the order of the error in Miles' expression for the pressure. For the case $U_{\mathrm{w}} \equiv 0$, assuming the expressions for the stream functions to be exact (though Miles obtained approximations), it is ϵ_{a}. For comparison, based on the assumption of infinite precision of the ϕ's, our expression for the pressure is correct to order $\delta\epsilon_{\mathrm{w}}^{-\frac{1}{2}}\epsilon_{\mathrm{a}}^{\frac{1}{3}}$ for $0.007 \leqslant \epsilon_{\mathrm{a}} \leqslant 0.02$ and to order $\delta\epsilon_{\mathrm{w}}^{-\frac{1}{2}}\epsilon_{\mathrm{a}}^{\frac{2}{3}}$ for $0.06 \leqslant \epsilon_{\mathrm{a}}$.

Another conclusion to be drawn from (19) is that, as growth by wind input and viscous damping nearly cancel, the growth rate of the gravity–capillary waves is very sensitive to slight changes of the oceanic and atmospheric parameters ρ_{a}, ρ_{w}, ν_{a} and ν_{w}.

3. Discussion of results

3.1. *Growth rates*

To calculate the growth rate numerically we neglect $\mathscr{T}$. This can be justified by noting that the leading term of $\mathscr{T}$ is of the same order as the error in $\mathscr{P}$ (as ϕ_{va} is correct to order $\epsilon_{\mathrm{a}}^{\frac{2}{3}}$). We use the following numerical values (all in SI): $g = 9.806$, $T/\rho_{\mathrm{w}} = 7.25\times10^{-5}$, $\delta = 1.2\times10^{-3}$, $\nu_{\mathrm{a}} = 1.5\times10^{-5}$ and $\nu_{\mathrm{w}} = 10^{-6}$.

In figure 2 the curves of the growth rate as a function of wavenumber are shown for several wind speeds. For $u_{*} \geqslant 0.05$ m/s all curves show a single positive maximum. We find a critical value for wave generation near $u_{*} = 0.05$ m/s. This value is in accordance with Miles (1962) and Kawai (1979*b*). For u_{*} between, roughly, 0.10 and 0.30 m/s the top of the curve occurs at such wavenumbers that $R_{\mathrm{a}} \simeq 36$. Growth at a certain wavenumber strongly increases with windspeed; there is no simple scaling law. The growth at the top of the curve increases even faster with increasing windspeed; this will be discussed later.

To compare our results with those of others we have chosen one specific friction velocity. The main features are the same for other values of u_{*}, which we have checked for $u_{*} \leqslant 0.4$ m/s. We find the same type of growth curves as Valenzuela (1976) and Kawai (1979*a*), as can be seen in figure 3. This implies that the decomposition of the stream function into a viscid and an inviscid part, which we have used throughout, is valid at all friction velocities; this point was left in doubt by Valenzuela (1976). The height of the top of our curve differs by about 10 % from that of Kawai and Valenzuela, in agreement with our estimated accuracy of $\epsilon_{\mathrm{a}}^{\frac{2}{3}} \simeq 7$ %. The difference between the curves of Kawai and Valenzuela is 20 %. As each curve is based on a different current profile these differences determine the sensitivity of the growth to small changes in the current profile. Miles (1962) studied smaller

† Miles studied the generalized situation of finite depth. We have taken the limit of his results for infinite depth and written his expression in our notation.

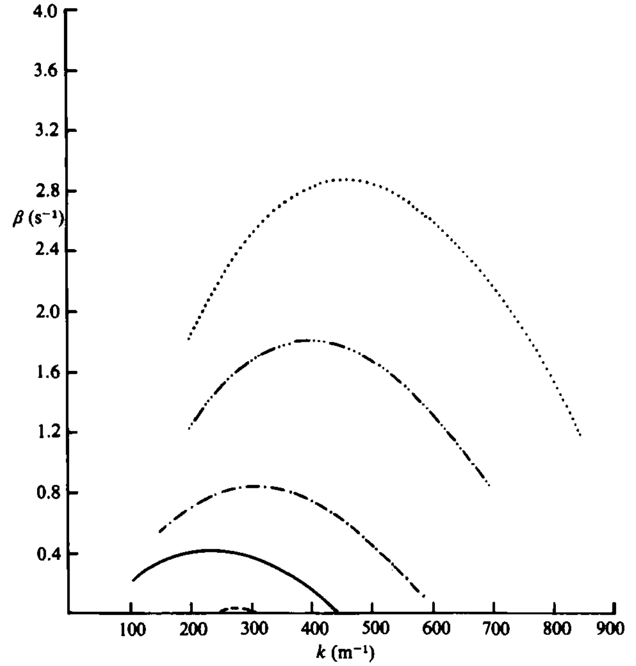

FIGURE 2. Growth rate as a function of wavenumber for various wind speeds: . . . . ., $u_* = 0.248$ m s^{-1}, $U_0 = 0.102$ m s^{-1}; —···—, 0.214, 0.098; —·—, 0.170, 0.096; ——, 0.136, 0.075; - - - -, 0.050, 0.025.

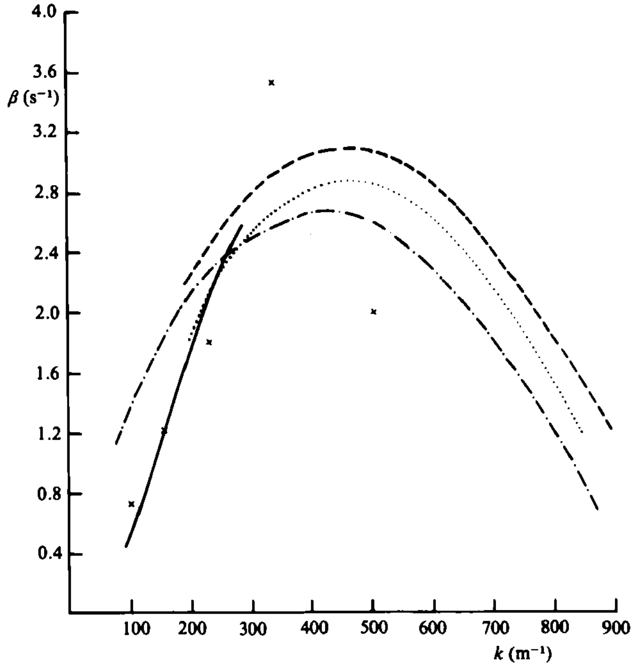

FIGURE 3. Growth rate as a function of wavenumber; a comparison between different studies, each using a different flow in water: ——, Miles (1962) $u_* = 0.23$ m s^{-1}; —·—, Valenzuela (1976) 0.25 m s^{-1}; - - - -, Kawai (1979*a*) 0.248 m s^{-1}; . . . . ., our study 0.248 m s^{-1}. Experimental results of Larson & Wright (1975) at $u_* = 0.27$ m s^{-1} are indicated with crosses.

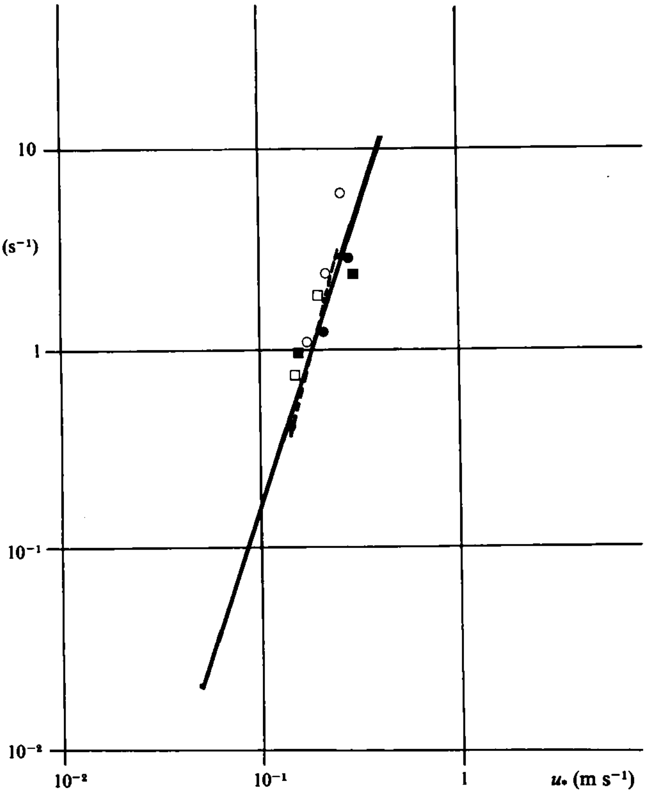

FIGURE 4. Maximum growth rate as a function of friction velocity. Theory: ■, Miles (1962); ●, Valenzuela (1976); – – – –, Kawai (1979*a*); —·—, our study. Measurements: □, Larson & Wright (1975); ○, Kawai (1979*a*).

wavenumbers than we have. Therefore not much more can be said than that the results of the two studies do not disagree. The measurements of Larson & Wright (1975) on β give values which are reproduced by our theory within 25 %.†

Those waves for which the growth rates are largest are the first to be generated by the wind (Kawai 1979). Therefore the maximum growth rates as a function of u_* are of interest and we have plotted them in figure 4. This plot also offers another method of comparing the effects of the various current profiles.

As a result of our calculations we find, for the range of friction velocities 0.05 m/s $\leqslant u_* \leqslant$ 0.4 m/s (roughly, this range coincides with 1 m/s $\leqslant U_{10} \leqslant$ 12 m/s), that

$$\beta_{\max} \approx u_*^3. \tag{24}$$

This is a surprisingly simple result considering the intricate expression (19*b*).

In the range considered we again find that our results are close to those of Miles, Valenzuela and Kawai; deviations are within 20 %. The values of the measurements

† There is some uncertainty concerning the friction velocity; Larson & Wright give the value u_* in the steady state while our computations are for the transient state. According to Kawai (1979*a*) u_* in the transient state is considerably less (up to 50 %) than in the steady state at the same value of, for instance, U_2. Another uncertainty is introduced by the fact that u_* determinations in the laboratory are, as a rule, exact up to not more than 5–10 %. However, we have neglected these complications and simply compared data at the same u_*.

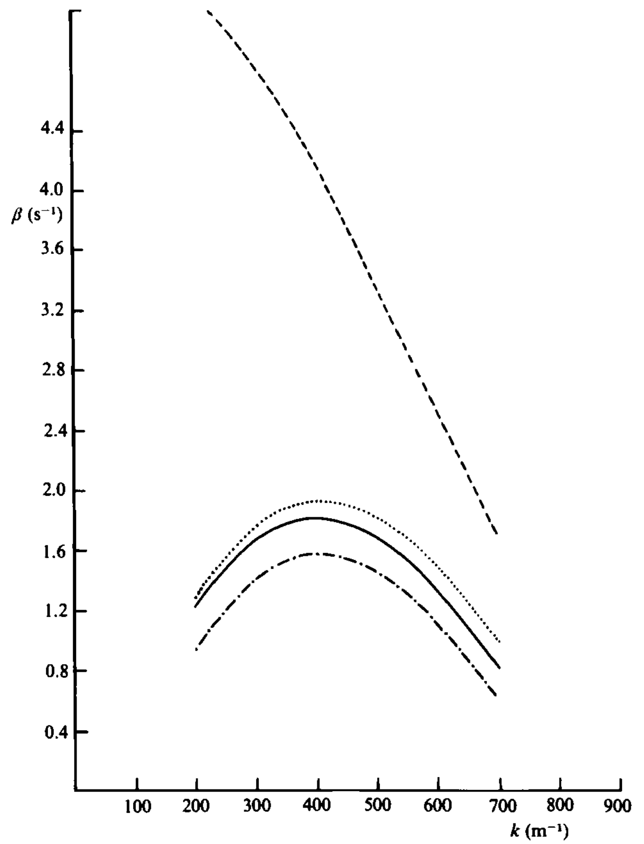

FIGURE 5. Growth rate as a function of wavenumber at $u_* = 0.214$ m s^{-1}, effect of changes in profiles: ——, our theory; - - - -, linear wind profile; —·—, $U_{\mathrm{w}} \equiv 0$; . . . . ., (25) as approximation to the pressure.

of Kawai and Larson & Wright are higher than the theoretical values; the largest difference is 100 % of the theoretical maximum growth rate. It must be noted that the functional dependence on u_* differs in the various theories and experiments; e.g. Kawai finds numerically that $\beta_{\max} \approx u_*^{3.5}$. Thus, for given u_*, β is independent of the current profile within 20 % but relation (24) is different for the various profiles.

To study the effect of the shape of the wind profile we have taken $r = 8$ (see (12)) and we have compared the linear–logarithmic profile with the linear profile (21). Note that these changes occur above the critical height. We have also studied separately the effects of the two features which distinguish Miles' theory from ours. We took a Benjamin type of approximation to the pressure – equal to $\mathscr{P}_{\mathrm{M}}$ to order ϵ_{a} – together with the exponential profile in water; that is, we used (19*b*) with $\mathscr{P}$ replaced by

$$\mathscr{P} = \frac{g}{ku_*^2\, W_0} + \lambda \tilde{U}_0 - W_0\, C\phi'_{\mathrm{iw0}} - \frac{[1/\epsilon_{\mathrm{a}} - W_0\,\phi'_{\mathrm{va}}]\,[1/\epsilon_{\mathrm{a}} - W_0\,\phi'_{\mathrm{ia}}]}{W_0(\phi'_{\mathrm{va}} - \phi'_{\mathrm{ia}})}. \tag{25}$$

Also we took $U_{\mathrm{w}} \equiv 0$ together with our expression for the pressure. The results for one value of u_* are shown in figure 5.

When the current is set uniformly equal to zero the growth rate becomes about 15 % lower than when the exponential profile is used. This deviation is in accordance with the sensitivity to the current profile we found above. When the linear wind profile is used we still obtain growth but the growth rates are incorrect. The results are best for high wavenumbers but even then the growth is two times too large. The growth curves as a function of wavenumber no longer show a maximum. When the linear–logarithmic profile is used with a thicker viscous sublayer, $r = 8$ instead of $r = 5$, growth is nearly, though not quite, $\frac{8}{5}$ times as much. When (25) is used for the pressure the growth corresponds within 20 % with the values found using our full expression for $\mathscr{P}$; the growth is always too large.

Our analysis shows that the growth is very sensitive to changes in the shape of the wind profile, even when these changes occur well above the critical height. This is not as surprising as it may seem. Miles (1957) was able to express the growth rate first in terms of an integral of the stream function and the wind profile from the interface up to infinity, and then in terms of values of these functions and their derivatives at the critical height (Miles 1957, p. 192: equations (4.1) and (4.2)). However, the stream function and its derivatives at the critical height still depend on all parts of the wind profile because the stream function is the solution of a differential equation containing this profile at all heights. Note that the second step of Miles as sketched above is not possible when viscosity is taken into account.

3.2. *Phase velocities*

In principle, the phase speed of the growing waves depends in two ways on the wind: directly; but also indirectly through the wind-induced current. First we treat the effect of the current. The current can be characterized by its value at the surface U_0 and by the shape of its profile. To study the effect of these two we have varied both. First, to investigate the effect of the shape of the current profile we compared our results with those of Valenzuela and Kawai using their values of U_0 and our profile. We find that the phase speed is insensitive to the choice of linear–logarithmic, exponential or Kawai's profile. Differences between values of the phase speed are in the order of a few percent. Using a constant profile, either $U_w \equiv 0$ or $U_w \equiv U_0$, leads to errors of about 20 % at $u_* = 0.136$ m/s and 50 % at $u_* = 0.6$ m/s.

As Valenzuela uses $U_0 = 0.8u_*$ while Kawai used his measured values, which are near $U_0 = 0.5u_*$, it is difficult to present illustrations of the foregoing in a figure. In figure 6 we show results for $u_* = 0{\cdot}136$ m/s: apart from Valenzuela's results all theoretical values are based on Kawai's value for U_0. Measurements of Kawai and Plant & Wright (1980) are also presented in figure 6. The effect of the value of U_0 depends on wavenumber and u_*. At higher wavenumbers the phase speed becomes less sensitive to U_0. For $k = 155\ \mathrm{m}^{-1}$ the dependence on U_0 for different friction velocities is shown in figure 7. At low friction velocities the influence of U_0 on c is small. However, at $u_* = 0.6$ m/s Valenzuela's value based on $U_0 = 0.8u_*$ is 50 % larger than our value, obtained by using $U_0 = 0.65u_*$. If we use $U_0 = 0.5u_*$ in our exponential profile we obtain a phase speed 40 % lower than that at $U_0 = 0.65u_*$. Using $U_0 = 0.65u_*$ our phase speeds compare well with the experimental data of Plant & Wright (1980), see figure 7. In their experiment U_0 was not measured: however they suggested $U_0 = 0.6u_*$. This analysis shows the importance of U_0 in comparing various theoretical methods and in comparing experimental and theoretical data.

Next we studied the direct effect of the wind. The wind has no direct effect on c_0 but has on c_1 (see (18) and (19)); the real part of c_1 is the first-order correction in δ, ϵ_a and ϵ_w on the phase speed. Thus the maximum possible direct effect is given by

$$\frac{c_1}{c_0} = O(\delta\epsilon_a^{-\frac{4}{3}}, \epsilon_w).$$

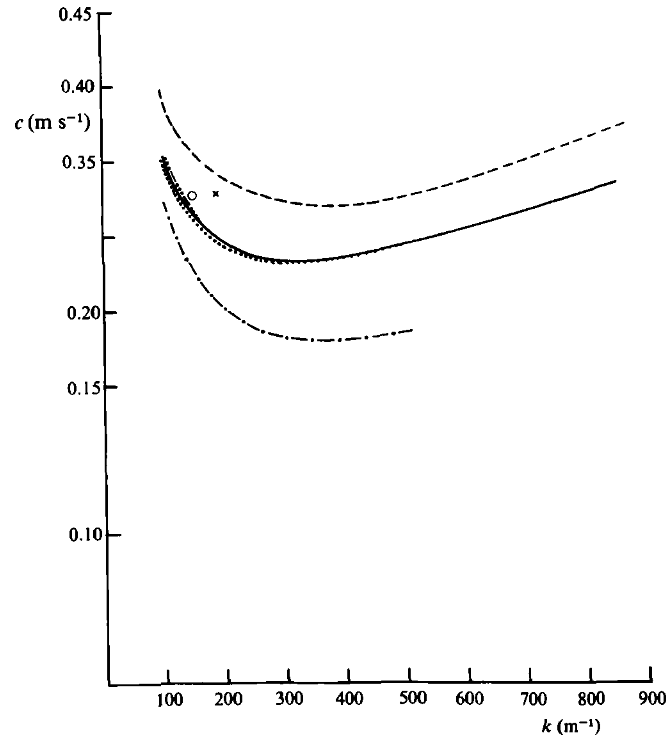

FIGURE 6. Phase velocity as a function of wavenumber at $u_* = 0.136$ m s^{-1}. Theory: ----, Valenzuela (1976); ....., Kawai (1979*a*); ——, our study, (19*a*); —···, our study, $\delta = 0$; —·—, our study, $U_w \equiv 0$. Measurement: ×, Kawai (1979*a*); ○, Plant & Wright (1980).

In practice $(1/c_0)\,\mathrm{Re}\,c_1$ is even smaller than this. For example, for $u_* = 0.136$ m/s and $100\ \mathrm{m}^{-1} < k < 500\ \mathrm{m}^{-1}$,

$$\frac{1}{c}\,\mathrm{Re}\,c_1 < 0.01 \quad (\delta\epsilon_a^{-\frac{4}{3}} < 0.04),$$

while for $u_* = 0.6$ m/s and $k = 700\ \mathrm{m}^{-1}$

$$\frac{1}{c}\,\mathrm{Re}\,c_1 = 0.16 \quad (\delta\epsilon_a^{-\frac{4}{3}} = 0.18),$$

and for $k = 155\ \mathrm{m}^{-1}$

$$\frac{1}{c}\,\mathrm{Re}\,c_1 = 0.30 \quad (\delta\epsilon_a^{-\frac{4}{3}} = 1.4).$$

Incidentally, $\mathrm{Re}\,c_1$ is always negative (see figure 7).

As well as this order analysis we have calculated the effect on the phase speed of changes in the shape of the wind profile by varying the thickness of the viscous sublayer; we compared $r = 5$ and $r = 8$. As is expected from the foregoing, for $u_* < 0.25$ m/s the difference is less than 1 % for all wavenumbers. For $u_* = 0.6$ m/s the difference is about 15 % of c (± 30 % of $\mathrm{Re}\,c_1$).

Summarizing, we can say that the wind-induced current has a large effect on the phase velocity; this can be 50 % of the phase speed of free waves. The exact shape of the profile – linear–logarithmic, exponential or Kawai's – is not of importance, though a constant profile leads to errors. However, the value of the current at the

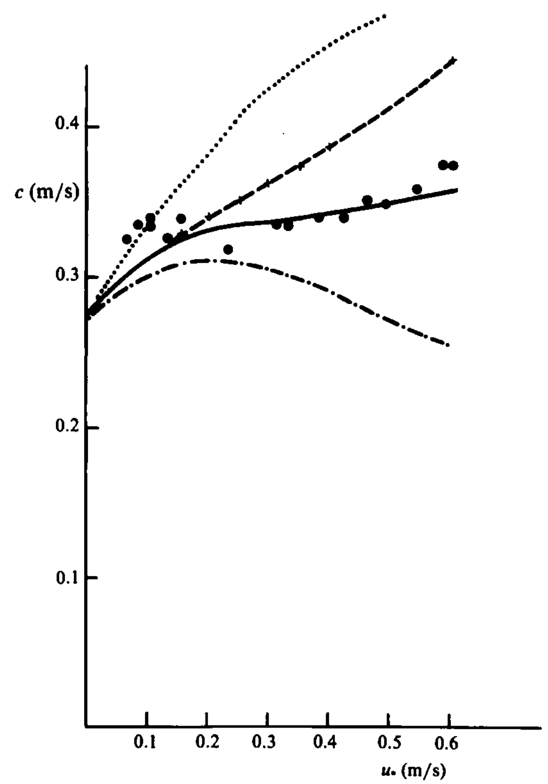

FIGURE 7. Phase velocity as a function of friction velocity for different values of U_0. Theory: . . . . ., Valenzuela (1976) $U_0 = 0.8u_*$; — —, our study: c_0, $U_0 = 0.65u_*$; ——, c, $U_0 = 0.65u_*$; —·—, c, $U_0 = 0.5u_*$. Measurements: ●, Plant & Wright (1980).

surface certainly is of importance, an error in U_0 of 25 % can lead to an error in the value of c of 50 %. This suggests that the value of the current and its shear at the surface are the two most important features of the current profile. The direct effect of the wind on the phase velocity is only noticeable at larger friction velocities: for $u_* = 0.6$ m/s it can be 15 % of c.

4. Main conclusions

It is possible to describe the initial growth of gravity–capillary waves with asymptotic methods. Our analysis results in expressions for phase velocity and growth rate accurate to order $\delta\epsilon_a^{-\frac{2}{3}}$ and $\epsilon_a^{\frac{2}{3}}$ respectively for $0.007 \leqslant \epsilon_a \leqslant 0.02$ and to order $\delta\epsilon_a^{-\frac{1}{3}}$ and $\epsilon_a^{\frac{2}{3}}$ respectively for $\epsilon_a \geqslant 0.06$, where ϵ_a is the inverse of a Reynolds number: $\epsilon_a = \nu_a k/u_*$. For intermediate ϵ_a the accuracy is also intermediate. Our analysis confirms the validity of Miles' (1962) expression for the growth rate.

Growing gravity–capillary waves are very sensitive to their environment. The wind speed strongly influences their growth; we find that the growth rate of the initial wavelets is proportional to u_*^3. There is no simple scaling law for the growth rate at fixed wavenumber but it also depends strongly on u_*. Changes in the shape of the wind profile, even above the critical height, can change the growth rate by a factor of more than three. The influence of the current profile on the growth is within ±20 %.

The phase velocity is more sensitive to the wind-induced current than to the wind itself; the effect of the current can be 50 % of the phase speed while the direct effect of the wind is less than 15 %. A linear–logarithmic, exponential or error-function-like profile all lead to the same results. Good agreement with experimental data can be obtained when the value of the current at the surface is known; errors in U_0 of 25 % lead to errors in c of up to 50 %.

Finally we checked that the perturbation normal pressure of the air on the surface causes the growth; the effect of the perturbation shear stress is an order $R_a^{\frac{1}{3}}$ smaller.

This work was partly supported by the Netherlands Organization for the Advancement of Pure Research (ZWO). We would like to thank G. R. Valenzuela for making his original data available to us, Anne de Baas and Wim Verkleij for comments on early versions of this paper, and Fred Dobson for an extensive review.

Appendix

$$\begin{aligned} K &= -\int_{-\infty}^{0} \frac{\phi_{\mathrm{iw0}}}{W}\left(\frac{\partial^2}{\partial\xi^2}-1\right)^2 \phi_{\mathrm{iw0}}\,\mathrm{d}\xi' \\ &= \frac{\lambda^3 U_0 c}{W_0^3 u_*^2} + \frac{\lambda^4 U_0^2}{c^3 F^2 u_*} \sum_{m=0}^{\infty} a_m \left(\frac{U_0}{c}\right)^m \\ &\times\left[\frac{2}{2+\lambda(m+2)} F\left(3, m+2+\frac{2}{\lambda}; m+3+\frac{2}{\lambda}; \frac{U_0}{c}\right)\right. \\ &\left.+\frac{U_0}{c(2+\lambda(m+3))} F\left(4, m+3+\frac{2}{\lambda}; m+4+\frac{2}{\lambda}; \frac{U_0}{c}\right)\right]. \end{aligned} \quad \text{(A 1)}$$

$$a_m = \left[\frac{\Gamma(r)}{\Gamma(p)\,\Gamma(q)}\right]^2 \sum_{j=0}^{m} \frac{\Gamma(p+j)\,\Gamma(q+j)}{\Gamma(r+j)\,j!}\,\frac{\Gamma(p+m-j)\,\Gamma(q+m-j)}{\Gamma(r+m-j)\,(m-j)!}. \quad \text{(A 2)}$$

Here and in the following F has p, q and r as parameters and U_0/c as argument when these are not specified.

$$\phi'_{\mathrm{iw0}}(0) = 1+\frac{\lambda U_0}{c}\frac{F'}{F}, \quad \text{(A 3)}$$

where a prime stands for differentiation with respect to the argument.

$$\mathscr{H} = -W_0\tilde{C}_1\phi'_{\mathrm{iw0}} - W_0 C\phi'_{\mathrm{iw1}} - \frac{1}{\mathrm{i}\epsilon_{\mathrm{w}}} W_0 \tilde{D}\phi'_{\mathrm{vw1}} + C(3\phi'_{\mathrm{iw0}} - \phi'''_{\mathrm{iw0}}) - \tilde{D}\phi'''_{\mathrm{vw}i}. \quad \text{(A 4)}$$

The terms $-(W_0/\mathrm{i}\epsilon_{\mathrm{w}})\,D\phi'_{\mathrm{vw0}}$ and $-D\phi'''_{\mathrm{vw0}}$ also appear in (A 4) but these cancel.

$$\mathscr{P} = \frac{g}{ku_*^2 W_0} + \lambda\tilde{U}_0 - W_0 C\phi'_{\mathrm{iw0}} + 3\mathrm{i}\epsilon_{\mathrm{a}} A\phi'_{\mathrm{ia}} - \mathrm{i}\epsilon_{\mathrm{a}}(A\phi'''_{\mathrm{ia}} + B\phi'''_{\mathrm{va}}). \quad \text{(A 5)}$$

$$\mathscr{T} = \epsilon_{\mathrm{a}} B\phi''_{\mathrm{va}}. \quad \text{(A 6)}$$

$$\mathscr{N} = C\phi'_{\mathrm{iw0}} - W_0 C\frac{\partial}{\partial c}\phi'_{\mathrm{iw0}} + \frac{1}{u_*^2 W_0^2}\left(\frac{g}{k}+\frac{Tk}{\rho_{\mathrm{w}}}\right). \quad \text{(A 7)}$$

$$m = \frac{-\mathrm{i}}{\epsilon_{\mathrm{w}}\phi''_{\mathrm{vw}}}\left(W_0\phi'_{\mathrm{iw0}} + W_0\phi'_{\mathrm{vw1}} + \mathrm{i}\epsilon_{\mathrm{w}}\phi'''_{\mathrm{vw1}}\right). \quad \text{(A 8)}$$

$$B = \frac{1}{W_0(\phi'_{\mathrm{va}} - \phi'_{\mathrm{ia}})}\left[\frac{1}{\epsilon_{\mathrm{a}}} - W_0\phi'_{\mathrm{ia}} + W_0\phi'_{\mathrm{iw0}} - \lambda\tilde{U}_0\right]. \quad \text{(A 9)}$$

$$A = 1-B. \quad \text{(A 10)}$$

$$D = \tilde{D} + \frac{\delta}{\phi''_{\mathrm{vw}}\epsilon_{\mathrm{w}}}, \quad \tilde{D} = \frac{1}{\phi''_{\mathrm{vw}}}(-1+\lambda^2\tilde{U}_0 - \phi''_{\mathrm{iw}}). \tag{A 11}$$

$$C = C_0 + \mathrm{i}\epsilon_{\mathrm{w}} C_1, \quad \frac{C_1}{C_0} = O(1). \tag{A 12}$$

$$C_0 = 1, \quad C_1 = \tilde{C}_1 + \frac{\delta}{\mathrm{i}\epsilon_{\mathrm{w}}^2 \phi''_{\mathrm{vw}}}, \tilde{C}_1 = \frac{1}{\mathrm{i}\epsilon_{\mathrm{w}}}\tilde{D}. \tag{A 13}$$

$$\phi'_{\mathrm{iw}1} = K. \tag{A 14}$$

$$\phi''_{\mathrm{iw}0} = 1 + \frac{\lambda^2\tilde{U}_0}{W_0}. \tag{A 15}$$

$$\phi'''_{\mathrm{iw}0} = \left(1+\frac{\lambda U_0}{c}\frac{F'}{F}\right)\left(1+\frac{\lambda^2\tilde{U}_0}{W_0}\right) + \frac{\lambda^3\tilde{U}_0}{W_0} - \frac{\lambda^3\tilde{U}_0^2}{W_0^2}. \tag{A 16}$$

$$\phi''_{\mathrm{vw}0} = \frac{-W_0}{\mathrm{i}\epsilon_{\mathrm{w}}}. \tag{A 17}$$

$$\phi'_{\mathrm{vw}1} = -\frac{5}{4}\frac{\lambda\tilde{U}_0}{W_0}. \tag{A 18}$$

$$\phi'''_{\mathrm{vw}1} = \frac{1}{\mathrm{i}\epsilon_{\mathrm{w}}}\tfrac{9}{4}\lambda\tilde{U}_0. \tag{A 19}$$

$$\phi'''_{\mathrm{ia}} = \phi'_{\mathrm{ia}} \quad \text{(at the surface)}. \tag{A 20}$$

$$\phi'_{\mathrm{va}} = \frac{\mathrm{i}^{\frac{1}{3}}}{\epsilon_{\mathrm{a}}^{\frac{2}{3}}}\,\mathrm{Ai}\,(\mathrm{i}^{\frac{1}{3}}\epsilon_{\mathrm{a}}^{\frac{1}{3}}W_0, 1) = \frac{-1}{\epsilon_{\mathrm{a}}^{\frac{2}{3}}D_{\mathrm{T}}(\epsilon_{\mathrm{a}}^{\frac{1}{3}}W_0)}. \tag{A 21}$$

$$\phi'''_{\mathrm{va}} = \frac{\mathrm{i}}{\epsilon_{\mathrm{a}}^2}[\epsilon_{\mathrm{a}} W_0 \phi'_{\mathrm{va}} - 1]. \tag{A 22}$$

$$\frac{\partial}{\partial c}\phi'_{\mathrm{iw}0} = \frac{\lambda U_0^2}{c^3}\left[-\frac{F''}{F} + \left(\frac{F'}{F}\right)^2 - \frac{c}{U_0}\frac{F'}{F}\right]. \tag{A 23}$$

$$\mathscr{P}_M = \frac{-(1/\epsilon_{\mathrm{a}} - W_0\phi'_{\mathrm{va}} + W_0)(1/\epsilon_{\mathrm{a}} - W_0\phi'_{\mathrm{ia}} + W_0)}{W_0(\phi'_{\mathrm{va}} - \phi'_{\mathrm{ia}})}. \tag{A 24}$$

This last expression is a translation of Miles' result into our notation; Miles did not substitute $U'_{\mathrm{a}} = u_*/\epsilon_{\mathrm{a}}$ and in his case $W_0 = -c/u_*$.

REFERENCES

ABRAMOWITZ, M. & STEGUN, I. A. 1965 *Handbook of Mathematical Functions*. Dover.

BATCHELOR, G. K. 1981 *An Introduction to Fluid Dynamics*. Cambridge University Press.

BENJAMIN, T. B. 1959 Shearing flow over a wavy boundary. *J. Fluid Mech.* **6**, 161–205.

DRAZIN, P. G. & REID, W. H. 1982 *Hydrodynamic Stability*. Cambridge University Press.

HOPF, L. 1914 Der Verlauf kleiner Schwingungen auf einer Strömung reibender Flüssigkeit. *Ann. Phys., Lpz.* (4) **44**, 1–60.

JANSSEN, P. A. E. M. & PEECK, H. H. 1985 On the quasilinear evolution of the coupled air-flow, water wave system. Submitted for publication.

KAWAI, S. 1977 On the generation of wind waves relating to the shear flow in water – a preliminary study. *Tôhoku University Series* 5, vol. 24, nos 1/2.

KAWAI, S. 1979*a* Generation of initial wavelets by instability of a coupled shear flow and their evolution to wind waves. *J. Fluid Mech.* **93**, 661–703.

KAWAI, S. 1979*b* Discussion on the critical wind speed for wind-wave generation on the basis of shear-flow instability theory. *J. Ocean. Soc. Japan* **35**, 179–186.

LARSON, T. R. & WRIGHT, J. W. 1975 Wind-generated gravity capillary waves: laboratory measurements of temporal growth rates using microwave backscatter. *J. Fluid Mech.* **70**, 417–436.

MILES, J. W. 1957 On the generation of surface waves by shear flows. *J. Fluid Mech.* **3**, 185–204.

MILES, J. W. 1962 On the generation of surface waves by shear flows, Part 4. *J. Fluid Mech.* **13**, 433–448.

MISES, R. VON 1912*a* Beitrag zum Oszillationsproblem. In: *Festschrift H. Weber*, pp. 252–282. Teubner.

MISES, R. VON 1912*b* Kleine Schwingungen und Turbulenz. *Jber. Deutsch. Math.-Verein* **21**, 241–248.

MONIN, A. S. & YAGLOM, A. M. 1971 *Statistical Fluid Mechanics: Mechanics of Turbulence*, vol. I. M.I.T. Press.

PLANT, W. J. & WRIGHT, J. W. 1980 Phase speeds of upwind and downwind travelling short gravity waves. *J. Geophys. Res.* **85**, 3304–3310.

RANEY, R. K., HASSELMANN, K., PLANT, J. W., ALPERS, W., SHUCHMAN, R. A., JAIN, A. & SHEMDIN, O. H. 1985 Theory of SCAR Ocean Wave Imaging: the Marsen Consensus, to be published.

VALENZUELA, G. R. 1976 The growth of gravity–capillary waves in the coupled shear flow. *J. Fluid Mech.* **76**, 229–250.

WHITHAM, G. B. 1974 *Linear and Nonlinear Waves.* Wiley.